Tutorial

Sven Schröder*, Alexander von Finck and Angela Duparré

# Standardization of light scattering measurements

DOI 10.1515/aot-2015-0041
Received September 4, 2015; accepted October 3, 2015; previously published online November 5, 2015

**Abstract:** In every advanced optical system, light scattering caused by the imperfections of optical components sooner or later becomes an issue that needs to be addressed. Light scattering can be a critical factor for both the throughput and the imaging quality of optical systems. On a component level, the quantities to describe these effects are the scatter loss or total scattering (TS) and the scattering distribution function or angle-resolved light scattering (ARS). In the last decades, a number of instruments have been developed worldwide for the measurement of TS and ARS. However, numerous pitfalls have to be avoided to obtain objective, reliable, and reproducible measurement results. This is, in particular, true for low scatter levels of high-end optical components. Standard procedures that have to be both concise and easy to implement are thus of crucial importance for the optics community. This paper tries to give an overview on existing standards as well as an outlook on new standards that are still being developed. Special emphasis is put on ISO standards jointly developed, reviewed, and revised by the international experts in the field.

**Keywords:** angle-resolved scattering; light scattering; roughness; total scattering.

## 1 Introduction

The low-level light scattering of optical components is both a well-known phenomenon and an issue that is difficult to understand in all detail and challenging to express in objective quantities. When light falls onto an optical component, such as a lens or a mirror, usually most of the light is transmitted or reflected into the specular directions. As a result of the interaction of the light with small imperfections, such as interface roughness, defects, or material inhomogeneities, however, a certain amount of light is scattered out of the specular directions. The amount and angular distribution of scattering depends on numerous parameters, such as the size of the imperfections, the dielectric properties, and the wavelength of light. Because of the complexity of the general scattering problem, predicting light scattering properties is challenging and direct measurements are indispensable.

The light scattering quantities of optical components can be divided into two major categories: angle-resolved scattering (ARS) and total scattering (TS). In this paper, an overview will be given on these quantities, their standardization, as well as the corresponding instrumentation. Examples of application are then given to illustrate the capabilities of standardized measurements.

Although high absolute accuracy and the low uncertainty of measurement are important issues, characterizing high-end optical components with particularly low scatter levels places some additional and special challenges. In particular, national metrology institutes strive for the highest accuracy and, among other things, provide important information on the scattering characteristics, for example, of white standard materials necessary for the traceable calibration of many radiometric instruments. Other laboratories, including Fraunhofer IOF, have special expertise in measuring scattering with highest sensitivities, which is indispensable for the characterization of high-quality optical components.

## 2 Definitions and standards

### 2.1 Scattering geometry

The most common scattering geometry used in the optics community is shown in Figure 1.

All angles are measured with respect to the sample normal. The incident beam hits the sample surface at

***Corresponding author: Sven Schröder,** Fraunhofer Institute for Applied Optics and Precision Engineering, Albert-Einstein-Str. 7, 07745 Jena, Germany, e-mail: sven.schroeder@iof.fraunhofer.de
**Alexander von Finck and Angela Duparré:** Fraunhofer Institute for Applied Optics and Precision Engineering, Albert-Einstein-Str. 7, 07745 Jena, Germany


© 2015 THOSS Media and De Gruyter

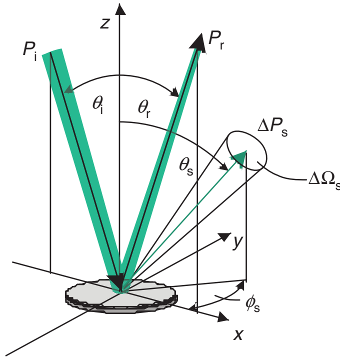


**Figure 1:** Scattering geometry.

an angle of incidence $\theta_i$. Part of the light is reflected into the specular direction $\theta_r$. $\theta_s$ and $\phi_s$ denote the polar and azimuthal angles of scattering, respectively.

## 2.2 TS

TS is defined as the power $P_s$ scattered into the forward or backward hemisphere normalized to the incident power $P_i$ [1]:

$$\mathrm{TS}=\frac{P_s}{P_i} \tag{1}$$

The procedures to measure TS are described in the international standard (ISO 13696) [1]. The standard also suggests the range of scattered radiation to be detected (range of acceptance angles) be $\theta_s = \leq 2°\ldots\geq 85°$ and $\phi_s = 0°\ldots 360°$ in the corresponding backward or forward hemispheres, although we usually even consider these limits to be not flexible but fixed. Total backscattering is denoted as $\mathrm{TS}_b$, and total forward scattering is denoted as $\mathrm{TS}_f$. TS is hence equivalent to the scattering loss of the component.

The well-defined range of acceptance angles is extremely important. It ensures that the specular beam is excluded from the measurement with a specific minimum scatter angle. If there was no such defined angular range, the measured TS would be extremely sensitive to the instrumental set-up used, in particular, when measuring high-quality optical components with most of the scattering concentrated around the specular directions.

Opaque as well as transparent samples can be measured. The influence of sample inhomogeneities is drastically reduced using the suggested procedure comprising a sample cross-scan, data reduction, and averaging. The ISO 13696 standard procedure was verified in an international round-robin experiment at 632.8 nm [2].

Another quantity, total integrated scattering (TIS), is still in use but should not be confused with TS. TIS is defined as the ratio of the diffuse reflectance $R_{\mathrm{diffuse}}$ to the total reflectance [3, 4]:

$$\mathrm{TIS}=\frac{P_{\mathrm{diffuse}}}{P_{\mathrm{diffuse}}+P_{\mathrm{specular}}} \tag{2}$$

Unfortunately, several optical design software codes use a definition of TIS that is essentially TS according to Equation (1), which has caused a lot of confusion.

A procedure for measuring TIS is prescribed in an ASTM standard [5]. One drawback of TIS is that it is defined for opaque but not transparent or semitransparent samples, such as substrates, AR coatings, and beam splitters. The more critical drawback, however, seems to be the undefined range of acceptance angles. More specifically, for a real sample, at which angle does the specular beam end and the diffuse scattering begin? Or, how to measure diffuse scatter within the specular beam?

We believe defining the range of acceptance angles or at least considering them is one strength of the ISO standard for TS. Another one is the proposed data reduction algorithm to suppress the impact of sample inhomogeneities and isolated defects onto the TS results.

Despite their practical differences, $\mathrm{TS}_b$ and TIS can theoretically be converted into each other if the reflectance $R=(P_{\mathrm{diffuse}}+P_{\mathrm{specular}})$ of the surface is known: $\mathrm{TS}_b = R_{\mathrm{TIS}}$.

Other quantities that are sometimes used as well are hemispherical directional reflectance (HDR), diffuse directional reflectance (DDR), and specular directional reflectance (SDR). $\mathrm{TS}_b$ can be approximated by DDR, and SDR corresponds to $R$, such that HDR should yield the sum of $\mathrm{TS}_b$ and $R$.

## 2.3 ARS

The scattering distribution basically describes the relative amount of light scattered into a certain direction. Many fundamental aspects of ARS measurements are described in ASTM standard E 1392 [6]. The procedure was verified in round-robin experiments at different wavelengths [7] but restricted to opaque samples. Later on, another ASTM standard has been established [8], which has a wider range of application.

Currently, an ISO standard procedure for ARS measurements is being developed by the International Working Group TC172/SC9/WG 6 of the ISO to meet the increased demands concerning wavelength ranges, sensitivity, flexibility, and practicability. All these standards basically describe the same quantity.

We define ARS as the power $\Delta P_s$ scattered into a given direction ($\theta_s$, $\phi_s$) normalized to the incident power $P_i$ and the solid angle of collection $\Delta\Omega_s$.

$$\mathrm{ARS}(\theta_s,\phi_s)=\frac{\Delta P_s(\theta_s,\phi_s)}{P_i\Delta\Omega_s} \quad (3)$$

$\Delta\Omega_s$ usually corresponds to the size of the detector aperture.

ARS is thus identical with the normalized radiometric (scattered) intensity. Other common terms used to express ARS are the bidirectional reflectance distribution function (BRDF) and the bidirectional transmittance distribution function (BTDF) referring to backscattering or forward scattering, respectively, or, more generally, the bidirectional scattering distribution function (BSDF). The main difference is that these functions are originally based on radiometric quantities and defined as the scattered radiance divided by the irradiance incident on a surface, which can then be rewritten as [9]

$$\mathrm{BSDF}(\theta_s,\phi_s)=\frac{dP_s(\theta_s,\phi_s)}{P_i d\Omega_s \cos\theta_s} \quad (4)$$

In real measurements, the detector solid angle as well as the measured power are finite quantities of course. Comparing Equations (3) and (4) thus suggests that BSDF and ARS are basically the same function, except for the cosine factor: BSDF=ARS/cos $\theta_s$. Because the cosine usually causes a steep increase of the scattering distribution at large scatter angles, it is often omitted. The resulting 'cosine-corrected' BSDF is identical with the ARS defined above. Some experts consider the BSDF as the fundamental quantity to describe scattering. Others, including the authors, prefer ARS, because this is the function that is actually measured. Nevertheless, both functions can easily be converted into each other when needed.

In the definition of ARS, normalizing to $P_i$ and $\Delta\Omega_s$ ensures that the measurement result does not depend on the specific instrument used, provided that measurements are performed at the measurement parameters, such as wavelength, location on the sample, or polarization states, and effects such as unelastic scattering and nonlinear effects can be neglected. Because the scattering across a sample can vary substantially depending on sample homogeneity and possible localized defects, the impact of the sample location should not be underestimated. This is, in particular, true for the high-quality samples with low intrinsic scatter levels. Therefore, this shall be addressed in the new ISO standard.

TS as defined in Section 2.2 cannot only be measured directly. Rather, it can be calculated by integrating the scattering distribution over the corresponding hemispheres:

$$\mathrm{TS}=\int_{0^\circ}^{2\pi}\int_{2^\circ}^{85^\circ}\mathrm{ARS}(\theta_s)\sin\theta_s d\theta_s d\phi_s \quad (5)$$

One big advantage of this approach is that ARS can be rather easily be measured at arbitrary angles of incidence and on curved samples, whereas the typical arrangements for TS measurements are more limited regarding sample geometries. However, a big advantage of TS measurements is the possibility to get quick TS scans of the entire sample area.

The question arises if TS determined through ARS can be regarded as TS according to the standard ISO 13696. However, based on the definition of both quantities and provided the instruments are calibrated correctly, the results should be comparable, as will be discussed in Section 4.

Finally, it is important to note that both quantities TS and ARS are often expected to represent a global or average property of a given sample. For a sufficiently homogeneous sample without localized defects, the results do not depend on the size of the illumination spot, which is usually in the range of a few millimeters. However, the scattering from localized defects such as particles, pits, or scratches depends on the size of the illuminating beam. Therefore, when characterizing defect scattering, another quantity, the differential scattering cross-section (DSC), has to be used [9]. For a single defect, DSC is simply ARS normalized to the area of the illumination spot: DSC=ARS$\pi D^2/4$, with $D$ being the beam diameter. These issues have to be kept in mind when analyzing light scattering data and should therefore be addressed in standards for light scattering measurements, although keeping standards simple yet concise is a challenging task.

## 3 Instruments for light scattering measurements and measurement procedures

### 3.1 TS

The instruments to measure TS (or TIS) are either based on integrating spheres (Ulbricht spheres) or Coblentz (collecting) hemispheres and have been developed in a number of laboratories [10–21].

Integrating spheres are coated with a diffusely scattering material, such as Spectralon™ (PTFE), barium sulfate, or rough gold, depending on the wavelength range of application. Inside the integrating sphere, the light scattered from a sample undergoes multiple scattering events leading to a homogeneous light distribution on the wall. A small part of the wall is taken by the entrance surface of the detector, either a photodiode or a photomultiplier tube (PMT). The small ration of the detector area compared to the total surface area of the integrating sphere limits the sensitivity of this set-up.

In contrast, Coblentz hemispheres are specularly reflective hemispherical mirrors that focus the light scattered from the sample directly onto the detector. Because basically all the light scattered hits the detector, Coblentz hemisphere-based instruments usually offer substantially higher sensitivities. Another advantage is that only a small volume around the sample is imaged onto the detector. This significantly reduces the impact of Rayleigh scattering of the specular beams on air molecules onto the measurements and thus offers lower detection limits.

Either way, in TS instruments according to the ISO standard, radiation propagating within 2° from the specular directions leave the integrating sphere or the Coblentz hemisphere without being detected. This is one precondition for system-independent results.

Figure 2 shows the schematic pictures of a TS arrangement based on an integrating sphere (left) and a Coblentz hemisphere (right), both in backscatter ($TS_b$) mode. To measure forward scattering in the case of the integrating sphere, the sample has to be placed at the other port of the sphere. In contrast, the instruments based on Coblentz hemispheres built at Fraunhofer IOF are designed such that switching to forward scatter mode is performed simply by flipping the entire set-up comprising the hemisphere, sample, and detector units.

With the Coblentz hemisphere-based instrument described in detail in Ref. [13], total backward and forward scattering are detected according to the instructions in the international standard ISO 13696 at wavelengths between 325 nm and 10.6 µm using several laser sources. The laser beam is prepared in the illumination system using a spatial filter (Figure 3). The incident beam hits the sample surface at nearly 0° and the specularly reflected beam is guided back through the entrance/exit port of the Coblentz hemisphere. The detector unit consists of a PMT for UV-VIS-NIR wavelengths or a cooled HgCdTe element for measurements in the IR located in a small integrating sphere for the homogeneous illumination of the detector area. The sample positioning system enables 1D and 2D scanning of the sample surface. By carefully adjusting the beam preparation system to suppress parasitic stray light, extremely low background levels as low as $5\times10^{-8}$ at 632.8 nm can be achieved [17].

The special instruments for TS measurements at VUV/DUV wavelengths below 200 nm were presented in Refs. [22–25].

One of the most important steps in measuring TS is calibration. TS could simply be calculated by dividing the corresponding detector signals when measuring scattered light or the direct incident beam deflected onto the detector. However, this would neglect the nonperfect transfer behavior of the Coblentz hemisphere or integrating sphere. It would also place even more stringent demands on the dynamic range and linearity of the detection system, because the signals of diffuse scattering of high-quality optical components is usually many orders of magnitude smaller than the signal corresponding to the

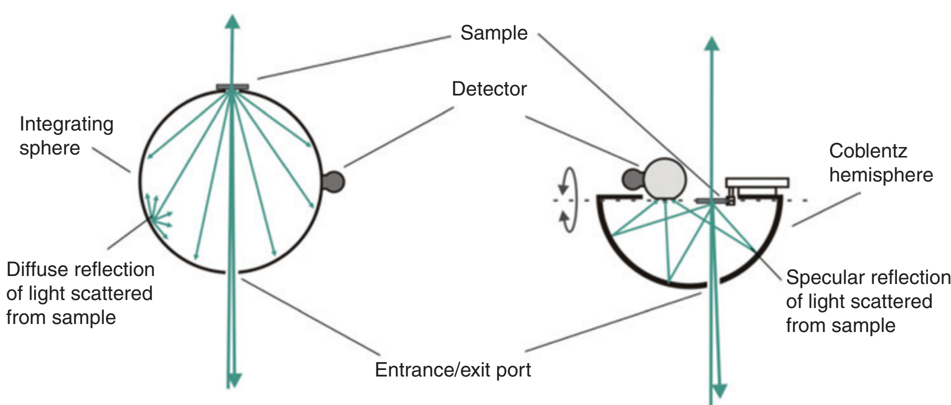


**Figure 2:** Set-ups for the measurement of TS. Left, Ulbricht (integrating) sphere; right, Coblentz (collecting) hemisphere. Both shown in backscatter mode.

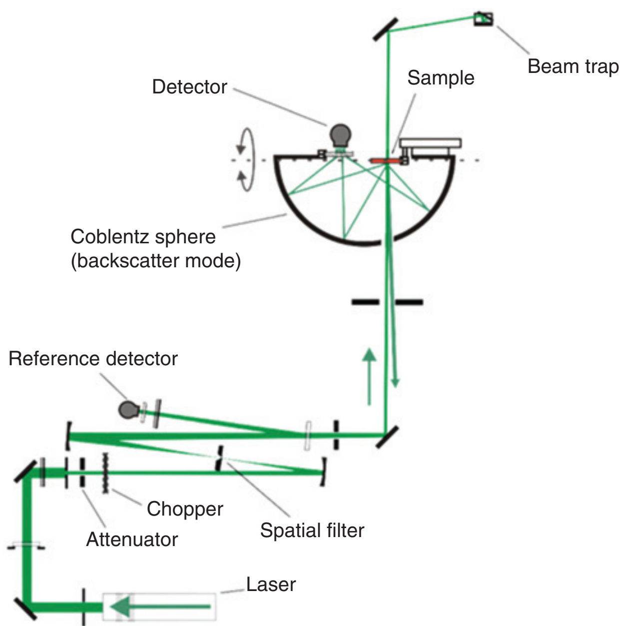


**Figure 3:** Instrument for total scatter measurements.

incident power. Therefore, calibration is performed using a diffuse scattering standard with known total reflectance. For the UV-VIS spectral regions, pressed PTFE powders, such as Spectralon™, are commonly used, whereas calibration in the IR is usually based on highly reflective diffuse gold. The total scatter is then determined by comparing the detector signals when measuring the sample $U_{\text{sample}}$ and the calibration sample $U_{\text{cal}}$:

$$\text{TS} = \frac{U_{\text{sample}}}{U_{\text{cal}}} C_{\text{cal}} \tag{6}$$

The calibration factor $C_{\text{cal}}$ corresponds to the total reflectance of the diffuse reflectance standard, which is usually certified by national metrology laboratories and for (white) Spectralon about 99.9%.

At wavelengths below 200 nm, no diffuse standards are available, so far. Therefore, measurements cannot be calibrated strictly according to the standard procedure. Yet, in Ref. [25], a method is presented that allows for calibrating TS measurements at 193–157 nm using a calcium fluoride diffusor whose TS is determined independently using ARS measurements at 193 nm and numerical integration. This or alternative approaches might be implemented in the future versions of ISO 13696. Although considerations exist that, in particular, for optical components with strong near-specular scattering, it might be more accurate to use calibration samples with more specular scattering characteristics. The goal of standardized measurements is, however, not only to achieve highest accuracy but also high reproducibility and comparability of different laboratories.

The typical procedure for total scatter measurements comprises:

- Careful alignment of the instrument
- Calibration of the instrument by measuring the scatter signal of a known reference sample (according to ISO 13696, diffuse reflectance standard)
- Verification of instrument performance by measuring background signature (without sample) and, if possible, measurement of known reference samples
- Measurement of sample, ideally by performing a lateral cross-scan followed by data reduction to reduce the impact of localized defects onto the average scatter signal

In addition to the final TS value, the report of the measurement data should list all parameters used during measurement as well as additional observations made on the sample, such as the presence of obvious defects or contaminations.

## 3.2 ARS

The measurement of ARS is mostly based on special goniophotometers, sometimes referred to as scatterometers. There are in-plane instruments, in which the range of detected scatter angles is confined to the plane of incidence, and 3D scatterometers that cover more or less the entire scattering sphere. In particular, ARS measurements of high-quality optical components require special instruments that go far beyond standard photogoniometers. Some of the requirements are

- High dynamic range (at least 11 orders of magnitude for VIS optics)
- Linearity over the entire dynamic range
- High sensitivity and low noise (noise level of $<10^{-6}$ sr$^{-1}$ for VIS optics)
- Small spectral bandwidth
- Small near-angle limit ($<0.5°$ for imaging applications)
- In the case of anisotropic scattering, the capability to measure not just in one plane but within the entire scattering sphere (3D scattering distribution)
- Capability to compensate for defocusing effects when measuring imaging components
- Sometimes, capability to characterize even large and complex components or entire systems
- Depending on the application: operation in clean room environment, high vacuum, purge gas, environmental monitoring/particle counting

Highly sensitive angle-resolved scatterometers have been set up in a variety of laboratories [10, 26–33]. The majority of such systems is designed for operation at visible light wavelengths, such as 632.8 nm (He-Ne laser), although special instruments exist that are capable of measuring ARS even in the IR and UV spectral regions [13, 17, 33–37]. Recent developments aim at spectral ARS measurements based on tunable laser sources [38–40].

Figure 4 shows the schematic principle of a 3D scatterometer for laser-based ARS, reflectance, and transmittance measurements in the UV-VIS-IR spectral regions. The instrument described in detail in Ref. [33] is located in a clean room to suppress light scattering from particles in the air and to avoid sample contamination.

Several lasers are used as light sources with wavelengths ranging from 325 nm to 10.6 µm. A chopper allows for lock-in amplification and noise suppression. Neutral density filters are used to adjust the incident power and to increase the dynamic range. The beam is focused by a spherical mirror onto a pinhole that acts as a spatial filter. The pinhole is then imaged by a spherical mirror over the sample onto the detector aperture. The last mirror can be translated to adjust the focal length of the illumination system. This is essential if measurements of curved samples are performed.

The sample is located on a positioning system to adjust the irradiated position and the angle of incidence. The instrument allows samples with diameters ranging from a few millimeters up to 670 mm to be investigated. Typical illumination spot diameters at the sample position are between 1 and 5 mm, although focusing to about 50 µm is also possible if required.

The detector, usually a PMT with lock-in signal processing, can be scanned within the plane of incidence (in-plane scatter measurement) or within the entire sphere around the sample (3D scatter measurement) to investigate the out-of-plane scattering of anisotropic samples. The diameter of the aperture in front of the PMT defines the detector solid angle $\Delta\Omega_s$. Aperture diameters between 0.1 and 5 mm are typically used depending on the specific requirements regarding sensitivity, speckle reduction, and near-angle limit. Up to 15 orders of magnitude dynamic range are achieved in the visible spectral range with the instrument shown. This is sufficient to investigate samples ranging from superpolished substrates with rms roughness levels below 0.1 nm, thin film coatings, optical materials, as well as nanostructured and technically rough surfaces.

Meanwhile, also compact tabletop instruments are available for ARS measurements that maintain key parameters, such as high sensitivity and high dynamic range, but are much smaller, easier to use, and can even be integrated into fabrication environments. A tabletop 3D scatterometer developed recently at Fraunhofer IOF [41, 42] is shown in Figure 5 (left). It allows for highly sensitive ARS measurements according to the standards. Another tool developed at Fraunhofer IOF is based on a CMOS matrix sensor rather than a scanning detector (Figure 5, right). This enables rapid 3D scattering measurements within a few seconds [43, 44]. However, although the instrument is calibrated and used according to the standards, it is not described in the existing standards. Nevertheless, it has been shown that the results obtained using this tool and standard scatterometers are in good agreement.

The careful calibration of scatter measurements is of crucial importance to compare results obtained with different instruments as well as to compare measurement with modeling results. The calibration of ARS measurements is performed either by measuring the incident power and the detector solid angle directly (absolute method) or by measuring the scattering of a diffuse reflectance standard with known ARS (relative method). Sometimes,

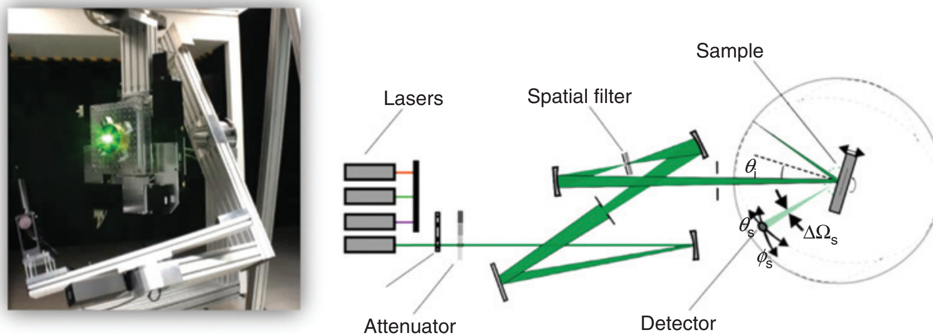


**Figure 4:** Left, set-up for ARS measurements; right, instrument ALBATROSS developed at Fraunhofer IOF for the measurements of optical components in the UV-VIS-IR regions.

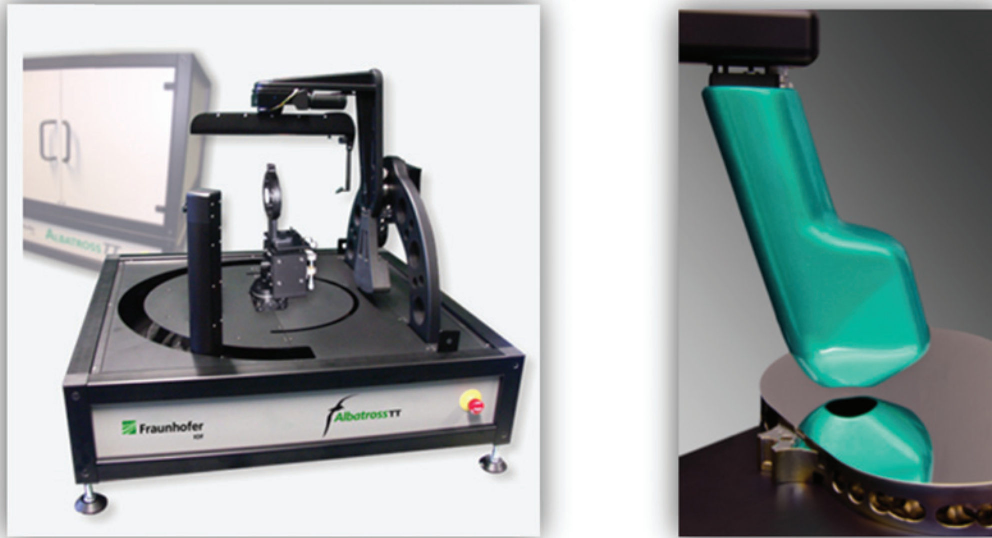


**Figure 5:** Tabletop and compact tools for ARS measurements. Left, scanning scatterometer ALBATROSS TT; right, CMOS-based scatter sensor Horos.

reference samples with known specular reflectance are used for instruments if the detector cannot be moved into the incident beam (however, see Section 4.4). Pressed PTFE powders, such as Spectralon™, are often used for this purpose in the UV-VIS range. They exhibit a nearly Lambertian ARS proportional to the cosine of the scatter angle (constant BRDF) with a maximum of about $1/\pi$ [9]. The relative method has the advantage of being less sensitive to system nonlinearity.

A typical procedure for ARS measurements comprises the following:

– Careful alignment of the instrument, including all axes, focus, and position of the illumination beam, as well as the field of view of the detector
– Selection of polarization conditions, angles of incidence and scattering, scanning resolution, and detector solid angles depending on the application
– Calibration of the instrument by measuring the scatter signal of a known reference sample (diffuse reflectance standard)
– Verification of instrument performance by measuring instrument signature (ARS scan without sample) and, if possible, measurement of known reference samples
– Alignment of the sample and definition of measurement spot(s) on the sample, for example, after performing a lateral sample scan with fixed scatter angle to identify homogeneous regions
– Measurement of the sample by performing a detector scan as given by the task

In addition to the resulting ARS curve(s) and the corresponding instrument signature, the report of the measurement data should list all parameters used during measurement as well as additional observations made on the sample, such as the presence of obvious defects or contaminations.

## 3.3 Uncertainty analysis of ARS and TS measurements

The main sources of uncertainty in scatter measurements are, of course, power fluctuations of the light source, detector noise (shot noise and excess noise of PMTs), calibration errors, and residual nonlinearities in the detection system. The estimation of the uncertainty of scatter measurements using the instrumentation developed at Fraunhofer IOF was performed according to the 'Guide to the estimation of uncertainty in measurement' [45] using a Monte Carlo method.

For ARS, simulations have shown that also the alignment of the instrument significantly contributes to measurement uncertainty. As a result, the uncertainty of ARS measurements is not constant over all scatter angles (Figure 6). It is dominated by alignment errors at very large angles and close to the specular directions where the steep in the ARS is very high [46]. The contribution of signal noise is a function of different signal adaption techniques and increases with smaller signal levels.

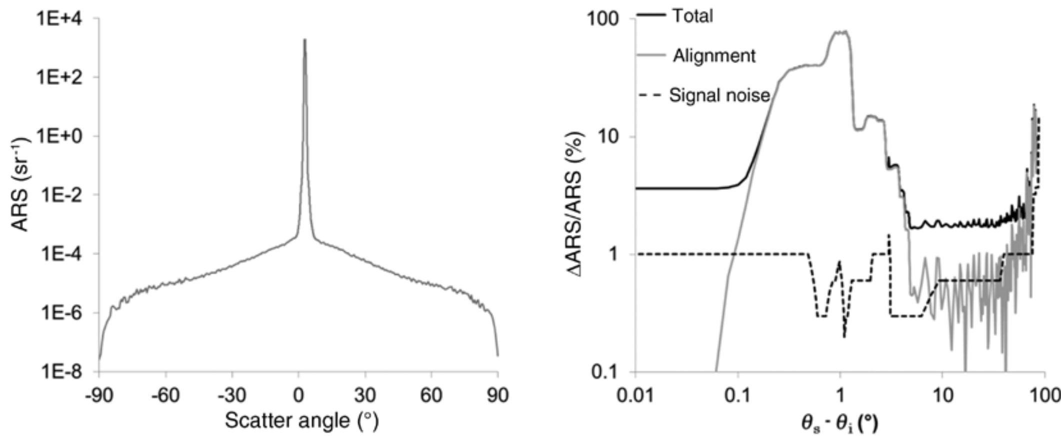


**Figure 6:** ARS measurement uncertainty analysis of a typical sample. Left, ARS measurement of an aluminum-coated substrate; right, contributions of signal noise and alignment uncertainty to the total measurement uncertainty.

Typical relative uncertainties are in the range of 10% but can be reduced to <5% under certain circumstances. Another yet less critical issue is the mechanical accuracy of goniometric instruments, which can be in the range of 0.01°, although the actual reproducibility as well as gravity-induced distortions of the measurement arms have to be taken into consideration as well. Also, a certain part of the backscattering hemisphere is usually not accessible because the detector head will obstruct the incident beam. In the instruments described in Refs. [33, 42], this obstruction area is minimized by using a small mirror to direct the scattered light into the detector system.

For TS, also the transfer behavior of the Coblentz hemisphere contributes to the uncertainty. Systematic studies have shown that a pessimistic estimation of the typical uncertainty is in the range of 15%. Yet, even this uncertainty means an extremely high accuracy when measuring the scatter loss of optical components. For example, for a laser mirror with a total scatter loss of 10 ppm, a relative uncertainty of 10% means an absolute uncertainty of only 1 ppm.

Finally, when discussing measurement uncertainty, one probably even more critical issue needs to be considered. For real samples, the variation of the scattering properties across the sample surface is often much larger than the actual uncertainty of measurement. This aspect has not been taken into account in existing standards for ARS measurements so far and should be addressed in future standards. In the new standard for ARS currently discussed in the ISO committee, a procedure shall be recommended (similar to the data reduction algorithm described in ISO 13696) to identify a location on the sample, which leads to results that are most representative for the average scattering properties of the entire sample.

# 4 Results and discussions

## 4.1 Instrument signatures

As discussed in Section 3, instrument signatures measured without any sample present are crucial to assess the results of light scattering measurements. Typical instrument signatures measured using the instrument ALBATROSS developed at Fraunhofer IOF are shown in Figure 7.

Plotted in Figure 7 is the ARS as a function of the scattering angle with 180° defined as the position of the directly transmitted incident beam. Thus, the shape of the peak at 180° reveals the functionality of the beam preparation system. The peak value corresponds to $1/\Delta\Omega_s$, the

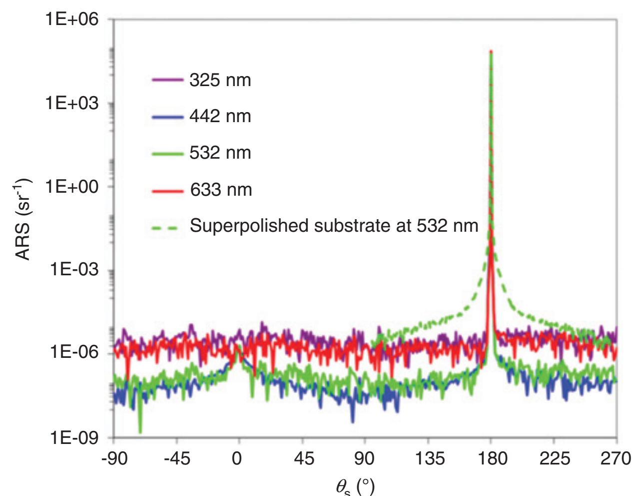


**Figure 7:** Instrument signatures for instrument ALBATROSS at different wavelengths.

effective solid angle covered by the detector aperture (for detector apertures larger than the specular beam). The signal about 0° corresponds to the backscattering of the beam trap for the transmitted beam. The residual scatter signal in the off-specular directions has three possible causes: (i) electronic noise of the detection system, (ii) Rayleigh scattering in the laboratory atmosphere, and (iii) residual stray light in the laboratory or instrument housing. The curves in Figure 7 clearly indicate that, at 442–532 nm, the instrument sensitivity is limited only by Rayleigh scattering, whereas, at 325–633 nm, because of the limited intensity of the light sources used, the sensitivity is limited by electronic noise. Meanwhile, Rayleigh limited performance has also been achieved with this instrument for 325 and 633 nm illumination.

The ratio between the highest signal (specular peak) and the lowest signals (noise floor or Rayleigh limit) is called dynamic range. For the characterization of optical components, dynamic ranges of more than 11 orders of magnitude and linearity over the entire dynamic range are required. This is illustrated by the scattering distribution of a superpolished substrate also shown in the diagram, which spans almost over the entire dynamic range of the instrument.

In Figure 8, the same data as shown in Figure 7 is shown but with a logarithmic scaling of the x-axis, revealing more details about the performance at small scattering angles.

The bumps in all signatures about 1° can be attributed to scattering from the components of the beam preparation system itself. It is interesting to note that, as one would expect, the background scattering is highest for

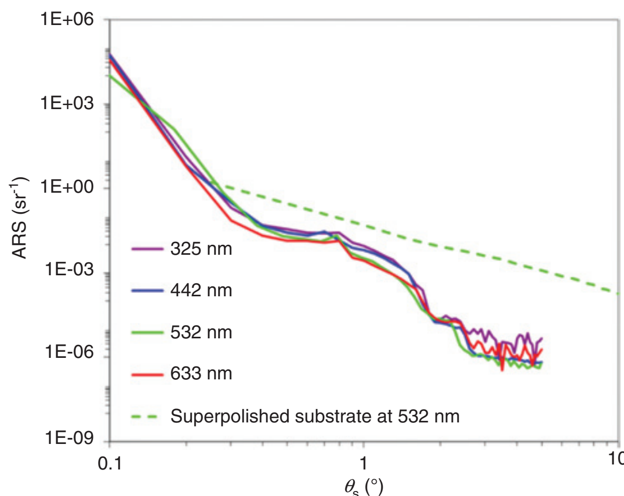


**Figure 8:** Same as Figure 7 but with x-axis on the logarithmic scale to show near-angle limits.

the shortest wavelength. Again, also plotted is the ARS of a superpolished substrate. The smallest scattering angle at which the scattering from the sample starts to get obstructed by the instrument signature is called the near-angle limit. The actual limit depends on the scattering properties of the sample under study. For the superpolished sample shown, the limit is about 0.2°. Retrieving information about the sample at smaller scatter angles is still possible but requires actively taking into account the signature.

Because the instrument signature is of such crucial importance, in particular, when analyzing the results of light scattering measurements of high-quality optical components, the requirement to provide a signature measured prior to the actual sample measurements should be part of the standard procedure.

## 4.2 Influence of defects and contaminations

Even high-quality optical components usually exhibit some inhomogeneities and local defects that can substantially influence the results of light scattering measurements. In Figure 9, the results of $TS_b$ mappings at 532 nm of a polished BK7 surface before and after cleaning using denatured ethanol and cotton batting are shown.

The average TS value before cleaning is $(8.7\pm29)\times10^{-6}$. The deviation stated is a measure for the fluctuations obviously caused by the impact of defects rather than an uncertainty of the measurement itself. After applying the data reduction algorithm prescribed in ISO 13696, a TS of $(7.3\pm0.4)\times10^{-6}$ is obtained. This value represents merely roughness-induced surface scattering as well as bulk scattering within the material by suppressing the impact of localized defects. The TS value after cleaning is $(7.6\pm0.3)\times10^{-6}$ and thus almost identical to the result obtained on the contaminated surface after applying the data reduction algorithm. This example clearly demonstrates the robustness of TS measurements when performed according to the standard procedure.

The example also illustrates the importance of considering inhomogeneities and defects when performing ARS measurements. In Figure 10, the results of ARS measurements at 532 nm of a superpolished silicon wafer are shown. The sample surface was first scanned at a fixed scatter angle of 15° to gather information about the homogeneity of the surface and possible contaminations and defects (Figure 10, left). The scatter map clearly reveals a considerable number of defects, most of which could possibly be removed by advanced cleaning methods.

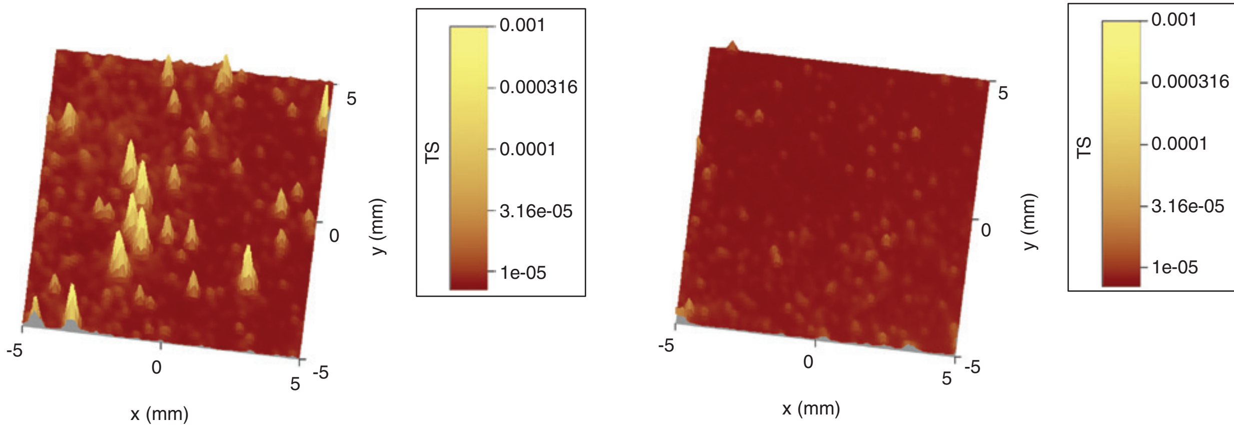


**Figure 9:** $TS_b$ mappings of polished BK7 surface before (left) and after (right) cleaning measured at 532 nm.

The rms roughness of the silicon wafer relevant for light scattering was determined using atomic force microscopy and PSD analysis to be as low as 0.16 nm. Because the roughness and thus the roughness-induced scattering of the sample is extremely low, even small defects lead to significantly increased scattering. The scatter signals at the defect sites in Figure 10 are about 2–3 orders of magnitude higher than the roughness-induced background. Therefore, if the intrinsic scattering distribution, not the defect scatter, shall be measured, a rather homogeneous low scattering region should be chosen for the measurement. The decision can be based on a scatter map or a linear sample scan. Figure 10 (right) shows the results of ARS scans at specific positions of the sample.

The roughness-induced scattering (A) is particularly low and close to but still above the sensitivity limit of the instrument. This is usually assumed to be intrinsic ARS of the sample. The $TS_b$ calculated by integrating the ARS curve is as low as $7.0\times10^{-8}$.

The scattering distribution at position B exhibits a fringe structure that is typical for the scattering from isolated particles that are larger than the wavelength used [47]. The particle diameter estimated by evaluating the positions of the first minima [48] is about 1.4 µm. The results demonstrate that even small particles significantly influence the results of scatter measurements. The influence becomes even larger when focusing onto the sample instead of the detector aperture. When scanning specifically for particles, a slight modification of the set-up is therefore used.

If the goal is to measure the average or intrinsic ARS of the sample, a surface scan should be performed prior to measurements to identify clean and homogeneous areas. The results also reveal that, for the proposed surface scan or scatter map, the choice of the (fixed) scatter angle is of crucial importance.

In Figure 11, the results of ARS scans at various positions on a superpolished EUV mirror substrate are shown [49, 50]. The surface has an extremely high quality, yet the scatter measurements clearly reveal some degree of unavoidable inhomogeneity caused by slight variations of surface roughness as well as small defects.

Most curves in Figure 11 are concentrated around a rather low average ARS. Only few curves are significantly higher and exhibit rather strong oscillations, indicating isolated defects. Analyzing the data at some arbitrarily chosen scatter angle in more detail reveals some interesting information, which is not obvious from the diagram. At $\theta_s$=-30°, the minimum ARS value is $2.2\times10^{-7}$ $sr^{-1}$, whereas the maximum value is $1.5\times10^{-6}$ $sr^{-1}$. The average ARS is $3.8\times10^{-7}$ $sr^{-1}$ with a relative standard deviation of as much as 74%. Applying a data reduction similar to the algorithm proposed in the standard for TS measurements leads to an average ARS of $3.1\times10^{-7}$ $sr^{-1}$ with a significantly lower relative standard deviation of 24%. This suggests that applying some sort of data reduction to suppress the impact of local defects on ARS measurements might be something that should be discussed in the standardization process. It is also interesting to note that the standard deviation even after data reduction is still higher than the relative uncertainty of ARS measurements discussed in Section 3.3.

## 4.3 Comparison of TS determined from ARS and TS measured directly

As discussed in Section 3, TS can either be measured directly using one of the methods described in Section 3.1 or determined by measuring ARS followed by numerical integration. The latter approach offers much more

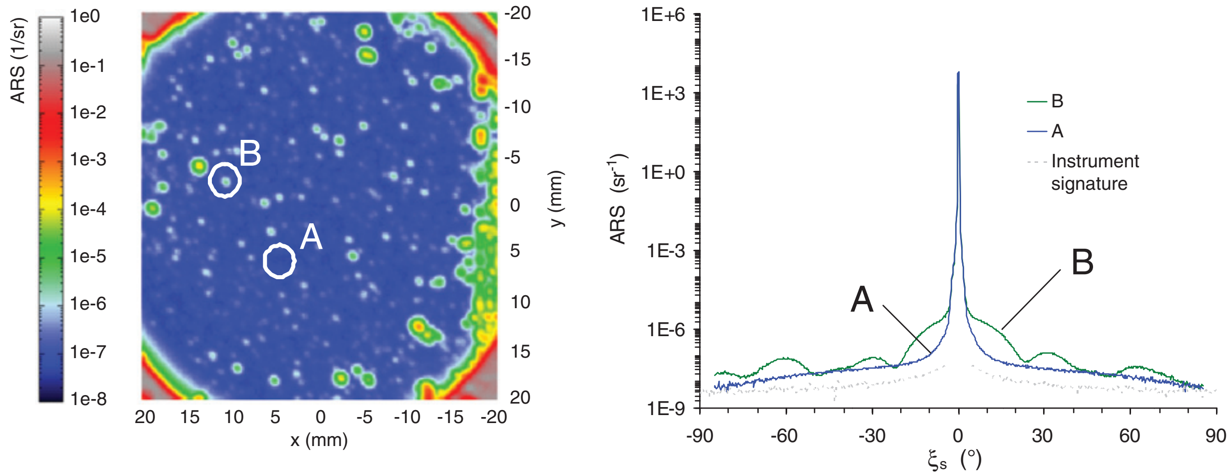


**Figure 10:** Results of ARS measurements at 532 nm of superpolished silicon wafer. Left, mapping at a fixed scatter angle of 15°; right, ARS distribution at two distinct positions on sample revealing roughness-induced scattering (A) and scattering of a single particle (B).

flexibility regarding sample dimensions, curvatures, and angles of incidence. Another advantage is that this allows for determining TS even in spectral ranges where neither Coblentz hemispheres nor integrating spheres are available, such as in the extreme UV spectral range. It is, however, not a standardized procedure yet. Nevertheless, given correct calibration and control of potential sources of systematic errors, the results should be comparable. A verification of this approach was performed on dielectric coatings for 157 nm.

The need for low scattering optical components for the deep UV spectral range, especially at 193–157 nm, is mainly driven by the developments of lithographic systems for the semiconductor industry and material processing applications. Because of the strong wavelength dependence of light scattering, even components with roughness levels of about 1 nm can easily produce light scattering of several percent (TS). At the same time, metal fluorides are the main choice as low-absorbing coating materials but cannot easily be deposited using high-energy processes such as ion-assisted deposition. As a result, DUV coatings tend to grow in columnar structures with enhanced roughness and porosity finally leading to significant light scattering.

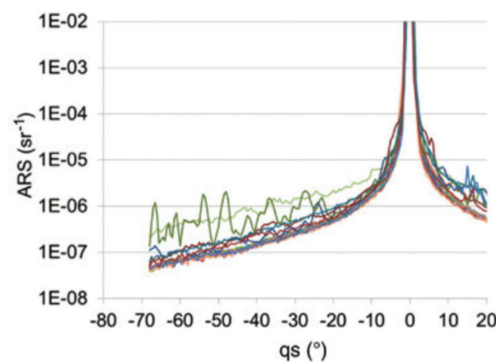


**Figure 11:** Results of ARS measurements of superpolished EUV mirror substrate at various positions.

The results of ARS and TS measurements in the backward direction of highly reflective multilayer coatings for 157 nm measured using the instrument discussed in detail in Ref. [25] is shown in Figure 12. The design of the coatings was $(LaF_3/AlF_3)^m/LaF_3$. Coatings with increasing numbers of layer pairs ($m$=5, 10, 15, and 25) were deposited on superpolished calcium fluoride substrates (rms roughness $\sigma$<0.2 nm) using thermal boat evaporation.

The ARS measurements were performed on a homogeneous area of the samples with an illumination spot diameter of 2 mm. The TS measurements were carried out as 1D scans across the sample surfaces. Both methods reveal a gradual increase of the scatter levels with the number $m$ of layer pairs. This can be explained by both the increasing interface roughness and the increasing reflectance of the coatings. The ARS curves provide more detailed information about the inner structure of the coatings, as discussed in detail in Ref. [33].

The total scatter (loss) can be calculated from the ARS curves through numerical integration. On the contrary, the TS scans directly provide the TS values as well as information about the homogeneities of the samples. The TS scan for the sample with $m$=5 exhibits increased scatter levels near the center of the sample, which is the result of scattering from a defect. From the TS scans, average TS values were calculated after applying a data reduction algorithm following ISO 13696, which automatically suppresses the

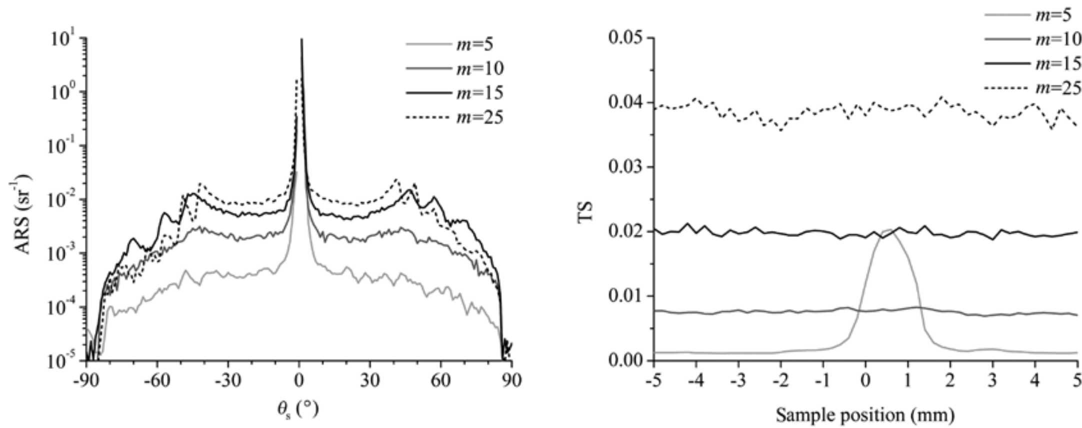


**Figure 12:** Results of ARS (left) and TS (right) measurements of highly reflective coatings at 157 nm with increasing number *m* of layer pairs.

influence of singular peaks. The average values are compared to the results derived by the integration of the ARS curves as shown in Table 1.

Even at this particularly challenging wavelength, there is a good agreement between the results. This clearly demonstrates the consistence of ARS and TS measurements when performed correctly. In particular, the well-defined ranges of integration and ranges of acceptance angles for the integration of ARS and measurement of TS, respectively, are crucial factors, as will be discussed in Section 4.4.

## 4.4 Explanation of deviations in specular reflectance measurements through ARS analysis

Many applications in laser optics require optical components with extremely high throughput corresponding to extremely low losses in the range of a few parts per million. Measuring the reflectance of high-end highly reflective mirrors is basically limited by the accuracy of the measurements, which hardly exceeds 0.1% of the actual reflectance. In contrast, direct measurements of the optical losses basically place challenging demands

**Table 1:** $TS_b$ values determined from ARS measurements compared to directly measured results.

| *m* | $TS_b$ from ARS | $TS_b$ measured |
|---|---|---|
| 5 | $1.4\times10^{-3}$ | $1.3\times10^{-3}$ |
| 10 | $8.1\times10^{-3}$ | $7.5\times10^{-3}$ |
| 15 | $2.8\times10^{-2}$ | $2.0\times10^{-2}$ |
| 25 | $3.1\times10^{-2}$ | $3.9\times10^{-2}$ |

on sensitivity, which can easier be met using appropriate equipment. Moreover, when performing light scattering measurements, the fact that part of the light is redistributed out of the specular direction but may or may not be partially detected as specular light depending on the size of the detector is obvious. This is, however, often ignored in specular measurements.

Within an international round-robin experiment, highly reflective dielectric mirrors for 1064 nm were characterized in terms of specular reflectance and losses [51]. Sixteen layer pairs of $SiO_2$ and $Ta_2O_5$ were deposited on superpolished fused silica substrates using magnetron sputtering.

The specular reflectance was measured using spectrophotometry and laser ratiometry [52] with substantial deviations between the results. ARS measurements were performed to verify the results of the reflectance measurements and to explain deviations of the results from different instruments. The result of an ARS measurement performed at 1064 nm is shown in Figure 13.

The results reveal a significant effect of replicated substrate roughness at small scatter angles as well as fringes corresponding to resonant scattering from the multilayer. But more importantly, the ARS results provide a straightforward explanation for the systematic differences of the direct reflectance measurements: The total scatter loss calculated from ARS is as low as $7.2\times10^{-6}$ (7 ppm) when integrating from 2° to 85° according to ISO 13696. However, substantially different results can be obtained by varying the lower limit of integration as indicated in the figure. The lower graph shows TS when calculated from ARS using different lower limits of integration. We usually specify TS according to ISO as the TS value resulting from integration from a scatter angle of 2°, which is the same as the minimum acceptance angle of our TS instruments. When

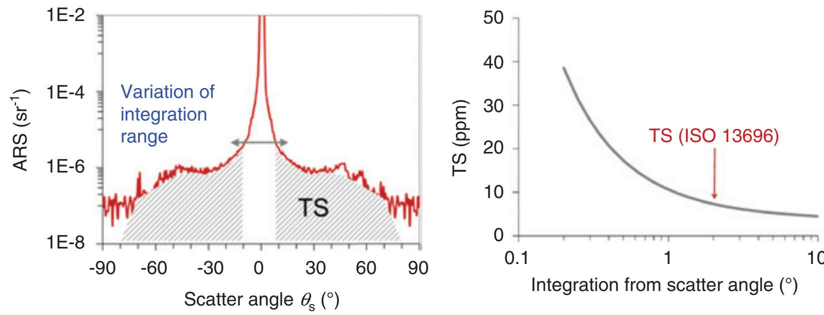


**Figure 13:** Results of ARS measurements of low-loss mirror at 1064 nm (left) and TS when calculated from ARS using different lower limits of integration (right).

integrating from 0.2°, the scatter loss increases to $38\times10^{-6}$ (38 ppm). This example illustrates that considering the ranges of acceptance angles is of crucial importance when measuring optical properties. Analyzing ARS data makes this process obvious and rather easy to handle. Yet, it seems to be neglected in the standards for specular reflectance and transmittance measurements so far [53, 54].

## 4.5 From in-plane to 3D ARS measurements

All results of ARS measurements were presented as in-plane data, so far, meaning that ARS is measured in one plane, the plane of incidence containing the sample normal and the incident beam. Providing these data is sufficient as long as the scattering of a given sample is isotropic and only depends on the polar not the azimuthal scattering angles. Many optical components, however, exhibit nonisotropic scattering. This can even be true for components such as polished surfaces or coatings, which are usually assumed to be perfectly isotropic. Clearly, non-isotropic scattering behavior can be expected from diffraction gratings, as significant parts of the incident light are redistributed from the specular directions into diffracted orders, which are usually oriented in one plane perpendicular to the grating structure.

The results of 3D scatter measurements in the forward (transmission) hemisphere of a diffraction grating at 532 nm performed using a 3D scatterometer [42] are shown in Figure 14. The diagram shows a top view on the transmission hemisphere. The distinct diffraction peaks can be clearly observed.

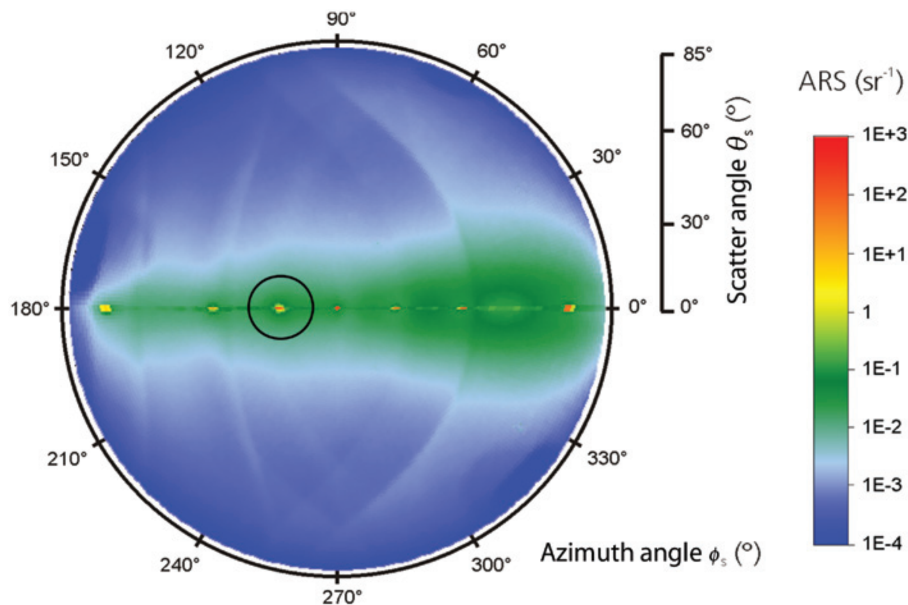


**Figure 14:** Results of 3D ARS measurements of diffraction grating at 532 nm in the transmission hemisphere. The black circle indicates the region of interest around the first diffracted order.

The figure also reveals significant out-of-plane scattering. A simple scan within the diffraction plane would not sufficiently reflect this behavior. As a matter of fact, the application required a certain level of integrated scattering around the first diffracted order in an angular range from 2° to 10° with respect to the direction of that order, as indicated by the black circle in the figure. The integration in this range yields an integrated scattering of $1.4\times10^{-3}$. In contrast, a scan in the diffraction plane utilizing a scatterometer without 3D capability would result in an overestimation of the integrated scattering by 1 order of magnitude ($1.6\times10^{-2}$). It has to pointed out that this is the quantity of interest for this application, although it is not a standard quantity. The example once more illustrates the advantage of ARS measurements – it provides detailed information on the scattering distribution and integral quantities, such as TS or fractional scattering, can easily be obtained.

## 5 Summary and conclusions

The accurate and reliable measurement of light scattering becomes more and more important to assess and verify the performance of optical components and to analyze imperfections and losses. Because of the numerous challenges involved in light scattering such as the requirements on sensitivity, dynamic ranges, calibration, and the influence of the instrument signature or extrinsic defects on the measurement results, standardized procedures are indispensable to obtain robust, reproducible, and comparable results.

TS describes the integrated scattering into either the reflective or the transmissive hemispheres. A standard procedure exists, which was proven to be extremely powerful in yielding robust results by suppressing the effects of surface inhomogeneities and localized defects. Moreover, TS explicitly considers ranges of acceptance angles, which turns out to be crucial when analyzing losses. TS should not be confused with TIS, which is still in use but has a slightly different definition.

ARS describes scattered power as a function of the scattering angles. Detailed descriptions of instrumentation and measurement techniques are available. A new standard procedure that should be concise yet simple is currently being developed within the ISO. TS can be calculated from ARS by numerical integration over the relevant range of scattering angles. If the scattering of a component is isotropic, a simple in-plane ARS scan is sufficient to calculate TS. In the case of anisotropic scattering, full 3D ARS measurements are necessary. The advantage of determining TS from ARS is that it can be done on arbitrary samples, plane and curved, small and large, and at arbitrary angles of incidence.

A variety of examples were discussed in this paper with the goal of illustrating the importance of standardized measurement procedures and their capabilities.

**Acknowledgments:** We are very grateful to Marcus Trost, Tobias Herffurth, and Matthias Hautpvogel (Fraunhofer IOF, Jena, Germany) for their contributions. The fruitful discussions with international experts in the field, such as Thomas Germer (NIST, Gaithersburg, MD) and John Stover (TSW, Tucson, AZ), are also highly appreciated.

## References

[1] ISO 13696, ‘Optics and Photonics – Lasers and Laser Related Equipment – Test Methods for Radiation Scattered by Optical Components’ (International Organization for Standardization, Geneva, Switzerland, 2002).
[2] P. Kadkhoda, A. Müller, D. Ristau, A. Duparré, S. Gliech, et al., Appl. Opt. 39, 3321–32 (2000).
[3] H. Davies, Proc. IEEE Part IV Inst. Monogr. 90, 209–214 (1954).
[4] H. Bennett and J. Porteus, J. Opt. Soc. Am. 51, 123–129 (1961).
[5] ASTM F 1048-87, ‘Standard Test Method for Measuring the Effective Surface Roughness of Optical Components by Total Integrated Scattering’ (American Society for Testing and Materials, Philadelphia, 1999).
[6] ASTM E 1392-90, ‘Standard Practice for Angle Resolved Optical Scatter Measurements on Specular or Diffuse Surfaces’ (American Society for Testing and Materials, Philadelphia, 1990).
[7] T. Leonhard and P. Rudolph, Proc. SPIE 1995, 285–293 (1993).
[8] ASTM E 2387-5, ‘Standard Practice for Goniometric Optical Scatter Measurements’ (American Society for Testing and Materials, Philadelphia, 2011).
[9] J. C. Stover, ‘Optical Scattering: Measurement and Analysis’ (SPIE Optical Engineering Press, Bellingham, WA, 2012).
[10] J. Bennett and L. Mattsson, in ‘Introduction to Surface Roughness and Scattering’, 2nd ed. (Optical Society of America, Washington, DC, 1999).
[11] H. Bennett, Opt. Eng. 17, 480–488 (1978).
[12] A. Duparré and S. Gliech, Proc. SPIE 3110, 566–573 (1997).
[13] A. Duparré, J. Ferré-Borrull, S. Gliech, G. Notni, J. Steinert, et al., Appl. Opt. 41, 154–171 (2002).
[14] D. Rönnow and E. Veszelei, Rev. Sci. Instrum. 65, 327–334 (1994).
[15] D. Rönnow and A. Roos, Rev. Sci. Instrum. 66, 2411–2422 (1995).
[16] O. Kienzle, J. Staub, and T. Tschudi, Meas. Sci. Technol. 5, 747–752 (1994).
[17] S. Schröder, S. Gliech, and A. Duparré, Proc. SPIE 5965 1B, 1–9 (2005).
[18] K. Guenther, P. Wierer, and J. Bennet, Appl. Opt. 23, 3820–3836 (1984).

[19] J. Detrio and S. Miner, Opt. Eng. 24, 419–422 (1985).
[20] A. Krasilnikova and J. Bulir, Proc. SPIE 5965, 59651I (2005).
[21] O. Balachninaite, R. Grigonis, V. Sirutkaitis, and R. Eckardt, Opt. Comm. 248, 15–25 (2005).
[22] P. Kadkhoda, A. Müller, and D. Ristau, Proc. SPIE 3902, 118–127 (2000).
[23] S. Gliech, J. Steinert, and A. Duparré, Appl. Opt. 41, 3224–3235 (2002).
[24] M. Otani, R. Biro, C. Ouchi, M. Hasegawa, Y. Suzuki, et al. Appl. Opt. 41, 3248–3255 (2002).
[25] S. Schröder, S. Gliech, and A. Duparré A. Appl. Opt. 44, 6093–6107 (2007).
[26] T. Germer and C. Asmail, Rev. Sci. Instrum. 70, 3688 (1999).
[27] P. Bousquet, F. Flory, and P. Roche, J. Opt. Soc. Am. 71, 1115–1123 (1981).
[28] J. Elson, J. Rahn, and J. Bennett, Appl. Opt. 19, 669–679 (1980).
[29] C. Amra, C. Grezes-Besset, P. Roche, and E. Pelletier, Appl. Opt. 28, 2723–2730 (1989).
[30] J. Neubert, T. Seifert, N. Czarnetzki, and T. Weigel, Proc. SPIE 2210, 543–552 (1994).
[31] F. Orazio, R. Silva, and W. Stockwell, Proc. SPIE 384, 123–132 (1983).
[32] C. Asmail, C. L. Cromer, J. E. Proctor, J. J. Hsia, and R. P. Division, Proc. SPIE 2260, 52–61 (1994).
[33] S. Schröder, T. Herffurth, H. Blaschke, and A. Duparré, Appl. Opt. 50, C164–C171 (2011).
[34] H. Hogrefe and C. Kunz, Appl. Opt. 26, 2851–2859 (1987).
[35] C. Amra, D. Torricini, and P. Roche, Appl. Opt. 32, 5462–5474 (1993).
[36] T. F. Schiff, M. W. Knighton, D. J. Wilson, F. M. Cady, J. C. Stover, et al., Proc. SPIE 1995, 121–130 (1993).
[37] M. Newell and R. Keski-Kuha, Appl. Opt. 36, 2897–2904 (1997).
[38] M. Zerrad, M. Lequime, and C. Amra, Proc. SPIE 8169, 81690K (2011).
[39] S. Schröder, M. Trost, T. Herffurth, A. von Finck, and A. Duparré, Adv. Opt. Technol. 3, 113–120 (2014).
[40] S. Schröder, D. Unglaub, M. Trost, X. Cheng, J. Zhang, et al., Appl. Opt. 53, A35–A41 (2014).
[41] A. von Finck, M. Hauptvogel, and A. Duparré, Appl. Opt. 50, C321–C328 (2011).
[42] A. von Finck, T. Herffurth, S. Schröder, A. Duparré, and S. Sinzinger, Appl. Opt. 53, A259–A269 (2014).
[43] T. Herffurth, S. Schröder, M. Trost, A. Duparré, and A. Tünnermann, Appl. Opt. 52, 3279–3287 (2013).
[44] T. Herffurth, M. Trost, S. Schröder, K. Täschner, H. Bartzsch, et al., Appl. Opt. 53, A351–A359 (2014).
[45] JCGM 100:2008, ‘Evaluation of Measurement Data – Guide to the Expression of Uncertainty in Measurement (GUM)’ (2008).
[46] A. von Finck, ‘Table Top System for Angle Resolved Light Scattering Measurement’, Dissertation (TU-Ilmenau, 2014).
[47] H. van de Hulst, ‘Light Scattering by Small Particles’ (John Wiley & Sons, New York, 1957).
[48] S. Maure, G. Albrand, and C. Amra, Appl. Opt. 35, 5573–5582 (1996).
[49] M. Trost, S. Schröder, T. Feigl, A. Duparré, and A. Tünnermann, Appl. Opt. 50, C148–C153 (2011).
[50] M. Trost, S. Schröder, A. Duparré, S. Risse, T. Feigl, et al., Opt. Express 21, 27852–27864 (2013).
[51] A. Duparré, D. Ristau, Appl. Opt. 50, C172–C177 (2011).
[52] S. Schröder and A. Duparré, Measurement of light scattering, transmittance, and reflectance, in ‘Laser-Induced Damage in Optical Materials’, Ed. By D. Ristau (Taylor & Francis, Boca Raton, 2013).
[53] ISO 15368, ‘Optics and Optical Instruments – Measurement of Reflectance of Plane Surfaces and Transmittance of Plane Parallel Elements’ (International Organization for Standardization, Geneva, Switzerland, 2001).
[54] ISO 13697, ‘Optics and Photonics – Lasers and Laser Related Equipment – Test Methods for Specular Reflectance and Regular Transmittance of Optical Laser Components’ (International Organization for Standardization, Geneva, Switzerland, 2006).